# An Accurate Analytical Model to Calculate the Impedance Bandwidth of a Proximity Coupled Microstrip Patch Antenna (PC-MSPA)

**NAFATI ABOSERWAL** [ID], (Member, IEEE),
**NIM R. CCOILLO RAMOS** [ID], (Student Member, IEEE),
**ZEESHAN QAMAR** [ID], (Member, IEEE),
**AND JORGE L. SALAZAR-CERRENO** [ID], (Senior Member, IEEE)
[1]Advanced Radar Research Center (ARRC), The University of Oklahoma, Norman, OK 73019, USA
[2]School of Electrical and Computer Engineering, The University of Oklahoma, Norman, OK 73019, USA

Corresponding author: Jorge L. Salazar-Cerreno (salazar@ou.edu)

**ABSTRACT** This paper presents a new set of analytical equations to calculate the impedance bandwidth of electrically thin and thick proximity-coupled square microstrip patch antenna (PC-MSPA). The proposed mathematical model uses the relationship among different antenna parameters, material, and antenna dimensions to estimate the percentage impedance bandwidth with high accuracy. The proposed model was validated with rigorous full-wave solutions, and experimental antenna prototypes implemented for different thicknesses, patch dimensions, frequencies, and different substrates. The theoretical bandwidth results of S-, C- and X-band PC-MSPA antennas obtained using the new model are in very good agreement with simulations and the experimental results. Errors between the proposed analytical model and both simulation and measurement are less than 3.1%. These equations are mostly valid for permittivities between 2.2 and 6.15, and with feed substrate thickness less than $0.1\lambda_r$. The PC-MSPA is a candidate element for integration with MIMIC devices and wireless communication applications.

**INDEX TERMS** Microstrip patch antenna, proximity coupling feed, wide bandwidth, multi-layer structure, non-linear curve-fitting technique.

## I. INTRODUCTION

Mmicrostrip patch antennas were first proposed by Deschamps in 1953 [1] and patented by Gutton and Baissinot in 1955 [2]. However, practical microstrip patch antennas were developed by Munson [3] and Howell [4] in the 1970s. Microstrip patch antennas have several well-known advantages over other conventional antennas; low cost, light weight, ease of manufacture, rugged, low radar cross-section, conformability, low production cost, compatibility with microwave integrated circuits, and capability to be easily formed into arrays [5]–[8]. These advantages make the microstrip patch antennas suitable for high performance aircraft, missiles, radars, satellite and mobile communication, radio frequency identification (RFID), global positioning system, space craft, and biomedical applications. However, a well-known inherent disadvantage of microstrip

patch antennas is their narrow impedance bandwidth that is typically a few percent because they are highly resonant structures. One of the important aspects of microstrip patch antennas is the variety of feeding techniques applicable to them. The comparison between those common feeding techniques is presented in [5]–[8]. The proximity-coupled microstrip patch antenna (PC-MSPA) is one of the printed antennas that provide a broadband, efficient solutions to integrating antennas with MIMIC circuits.

The proximity-coupled feeding technique, one of non-contact feeding methods, provides large bandwidth (as high as 13%) compared to other feeding techniques where there is a direct contact between the feed line and the radiating patch like a probe-fed and edge-fed methods [5]–[8]. In contrast to the direct contact methods, which are predominantly inductive, this feeding mechanism is capacitive in nature. This capacitive loading significantly affects the obtained impedance bandwidth, thus providing a wider bandwidth. In addition, this simple feeding technique provides

The associate editor coordinating the review of this manuscript and approving it for publication was Lin Peng [ID].

enhanced bandwidth without undesired radiation caused by the discontinuities and asymmetry of direct contact feed methods [5]–[8].

The modeling and analysis of a proximity-coupled microstrip patch antenna is difficult due to the complex electromagnetic interaction involved between the feed line and the radiating patch. Over the past decades, microstrip patch antennas have been analyzed extensively, employing a wide variety of analytical techniques, which are simple intuitive models with different levels of approximation as the transmission line model, the cavity model and segmentation model [9]–[13]. These models work well for thin, low dielectric constant substrate, but exhibit less accuracy at the substrate thickness and/or the dielectric constant increases. Some of the feed configurations such as proximity-coupled microstrip feed is difficult to model using the analytical techniques because the effect of the coupling capacitor between the microstrip feed line and the patch as well as the equivalent R-L-C resonant circuit representing the patch with two-layered substrate should be taken into account when designing the antenna. However, most of the analytical models' limitations can be overcome in the full-wave techniques. In [14]–[17], the most popular full-wave techniques such as the method of moments (MoM), the finite-element method (FEM), the spectral domain technique (SDT), the finite-difference time domain (FDTD) method have been used to analyze and design a proximity-coupled microstrip patch antenna. Although these numerical techniques maintain accuracy, completeness and versatility at the expense of numerical simplicity, they are difficult to implement due to extensive computational procedures.

In [18], graphical guidelines for design of proximity-coupled square and circle microstrip patch antennas are given. These graphical design curves are obtained by using a rigorous moment method formulation, employing the Green function for the double-layered structure. To the authors knowledge, there appears to be no overview on how to achieve broad impedance bandwidth for a double-layered proximity-coupled microstrip patch antenna and how its parameters affects the antenna bandwidth.

This paper proposes a mathematical-based analysis and a alternative design procedure that provides a solution for a PC-MSPA design. Therefore, the organization of this paper is as follows: A brief review of PC-MSPA is presented in Section II. Then, in Section III, described the proposed model in detail. In Section IV, four antenna prototypes were developed and tested to validate the proposed model. Section V, shows an error analysis of proposed model and comparison with other analytical expressions used for bandwidth estimation of conventional MS patch antennas.

## II. PROXIMITY-COUPLED MICROSTRIP PATCH ANTENNA (PC-MSPA)

The double-layered proximity-coupled square microstrip patch antenna shown in Fig. 1 is called electromagnetically coupled (EMC) microstrip patch antenna. This type of
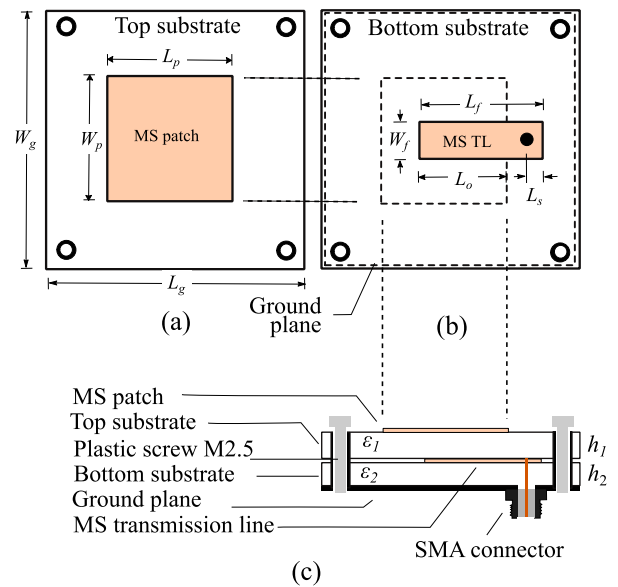


**FIGURE 1.** Geometry of the proximity-coupled square microstrip patch antenna (PC-MSPA). (a) Top view. (b) Mid-section of PC-MSPA, and (c) Stack-up definition of PC-MSPA.

feeding technique comes under non contacting scheme as there is no physical contact between the radiating patch and the feed line. As shown in Fig. 1, two substrates are used such that the feed line terminated with an open circuit is between the two substrates, the radiating patch with dimensions $L_p$ and $W_p$ is on top of the upper substrate and the lower (feed) substrate is grounded. The microstrip feedline of width $W_f$ is centered with respect to the patch width, and is inset a distance $L_0$ from the the edge of the patch.

Since no direct contact between the microstrip feed line and the radiating patch in this feeding mechanism, the radiating patch on the upper substrate (patch layer) is excited by an open-ended microstrip feed line printed on the lower substrate (feed layer) through capacitive coupling. Matching can be achieved by controlling the length of the feed line (feeding stub) and the width-to-line ratio of the patch. The coupling increases with feed inset reaching a maximum when $L_0 = L_p/2$. The coupling is symmetrical with respect to the center of the patch and can be increased by decreasing the patch width [19].

The main advantage of this feed technique is that it provides high bandwidth and eliminates spurious feed radiation, due to overall increase in the thickness of the microstrip patch antenna. In addition, this technique gives option to independently select the two dielectric substrates to further optimize both feed line performance and patch performance. However, the fabrication is bit complex which is a disadvantage.

Different approaches have been found in the state of technique that aims to analyze and optimize different parameters of microstrip patch antennas, such as the bandwidth, the cross-polarization level and the gain, based on full-wave solutions. Apart of the simulation-based techniques, two-layer PC-MSPA modeling has been approached

in the state of art, although its challenges and limited close models available so far. Considering the average permittivity [20] and its effective value, Parrikar and Gupta [21] developed a multi-port model making the two substrates be equivalent to a one-average substrate, which average electrical relative permittivity was calculated as follows:

$$\varepsilon_{av} = \frac{\varepsilon_1 \varepsilon_2 (h_1 + h_2)}{\varepsilon_1 h_2 + \varepsilon_2 h_1} \quad (1)$$

Besides, diverse studies have analyzed the microstrip patch antenna with different feeding strategies, seeking for an analytical expression of the bandwidth. Starting from different expressions of the bandwidth based on the VSWR [22], [23], Jackson and Alexopoulos [24] derived a closed form of the bandwidth for one-substrate microstrip patch antennas. This formula becomes increasingly inaccurate for thicker or multiple substrates. A different expression for calculating the percentage bandwidth of the rectangular MS patch antenna in terms of its dimensions and substrate parameters is described in [25]. In [26], another simplified relation for quick calculation of BW (in MHz) for VSWR = 2 of the MS patch antenna operating at frequency $f$ (in GHz), with $h$ expressed (in cm) is derived. However, this simple formula does not take in account the dielectric constant of the patch antenna substrate and it can be only used for low-$Q$ MS patch antenna with thin substrate.

Considering the average substrate permittivity expression in Eq. (1), Kumprasert et al. [27] developed a closed-form expression for the bandwidth in a prob-fed microstrip patch antenna. Following the bandwidth behavior, Parizi [28] described techniques to improve the bandwidth in MSPA. Among them, the intrinsic techniques aim to modify the antenna geometry, i.e. substrate thickness ($h$) and dielectric constant ($\varepsilon_r$), according to what was discussed in the prior paragraph. However, the author mentions that the counterpart of making an increase of $h$ and decreasing $\varepsilon_r$ affects the gain, increase the cross-polarization level and the spurious radiations. Therefore, not only geometry optimizations would be necessary to usefully increase the bandwidth, but also selecting the appropriate feeding technique and material dimensions that support the feeding. Referring particularly to the PC-MSPA, Parizi describes that the typical bandwidth ratio is about 8%, and an increase of this parameter can be obtained if increasing the thickness of the feeding layer, but being aware that more spurious radiation can be released. Another way to increase the bandwidth suggested is to make a matching structure in the port, i.e. a quarter-wave transformer between the input and the section that makes the coupling with the patch. In addition, other techniques have been used to enhance the bandwidth of electromagnetically coupled microstrip patch antennas by utilizing a tuning stub. In [19], a small tuning stub is connected in shunt with the feed line of the proximity coupled microstrip patch antenna to improve the impedance bandwidth. The similar approach with a dual-stub design has been used to increase the bandwidth from 4.8 to 8.4% in [29].

## III. PROPOSED DESIGN MODEL FOR THE PC-MSPA

This section describes a new set of equations derived based on non-linear regression procedure to estimate the bandwidth of the PC-MSPA, shown in Fig. 1. The antenna PC-MSPA is designed to operate at $f_o$, where the MS transmission line is used to excite the MS patch is located between the patch substrate and the feeding substrate. From Fig. 1, the respective thickness and relative permittivities are $h_1$, $\varepsilon_1$, $h_2$ and $\varepsilon_2$, from which the rest of dimensions can be obtained. From these dimensions, and assuming $\varepsilon_1 = \varepsilon_2 = \varepsilon_r$, the following variables are also defined in terms of guided wavelength ($\lambda_r = \lambda_o/\sqrt{\varepsilon_r}$), $h_{1_{\lambda_r}} = h_1/\lambda_r$, $R_h = h_2/h_1$, and $R_p = L_0/L_p$, which will be used in the model equations following later in this section. The following new model equations (3-29) of $R_p$, $R_h$ and %BW are obtained by applying the non-linear curve-fitting technique [30] to the full wave solutions.

### A. GEOMETRY OF THE PC-MSPA
The PC-MSPA design procedure aims to get the complete antenna geometry (substrates thicknesses, patch and feed transmission line dimensions) from the knowledge of the material (relative permittivity $\varepsilon_r$) and desired central frequency ($f_o$).

#### 1) FEED TRANSMISSION LINE
It is known that the impedance matching is produced by having a feeding transmission line with the appropriate width and length, since these dimensions are directly related to the characteristic impedance and electrical length, respectively.

The transmission line width $W_f$ can be set following the microstrip line design procedure [31] to get characteristic impedance $Z_0$ of 50 Ω, as $Z_0 = f(W_f/h_1, \varepsilon_r)$.

On the other hand, the length $L_f$ can be calculated as:

$$L_f = 0.5(L_g - L_p) + R_p L_p \quad (2)$$

The antenna matching can be set around the operating central frequency $f_o$ if the length portion of the feeding transmission line $L_0$ is a certain fraction of the patch length $L_p$. In that sense, the fraction $R_p$ can be calculated through the equations bellow and according to Fig. 1. These equations are illustrated in Fig. 2(a) with HFSS-simulated data and using the materials: Rogers[TM] 5880 Duroid ($\varepsilon_r = 2.2$), Rogers[TM] 4350B ($\varepsilon_r = 3.66$) and Rogers[TM] 6006 ($\varepsilon_r = 6.15$).

$$R_p = x_1 h_{1_{\lambda_r}}^3 + x_2 h_{1_{\lambda_r}}^2 + x_3 h_{1_{\lambda_r}} + x_4 \quad (3)$$

where $x_1$, $x_2$, $x_3$ and $x_4$ can be obtained using:

$$x_1 = 73.75\varepsilon_r^2 - 834.9\varepsilon_r + 3129 \quad (4)$$

$$x_2 = -149.9 - 257.1e^{-0.1708\varepsilon_r^2} \quad (5)$$

$$x_3 = 0.2772\varepsilon_r^2 - 2.489\varepsilon_r + 8.502 \quad (6)$$

$$x_4 = 0.89 \quad (7)$$

These equations are mostly valid for permittivities between 2.2 and 6.15, and with feed substrate thickness less than $0.1\lambda_r$ (265 mils in Rogers[TM] 5880 Duroid, 205 mils in Rogers[TM]
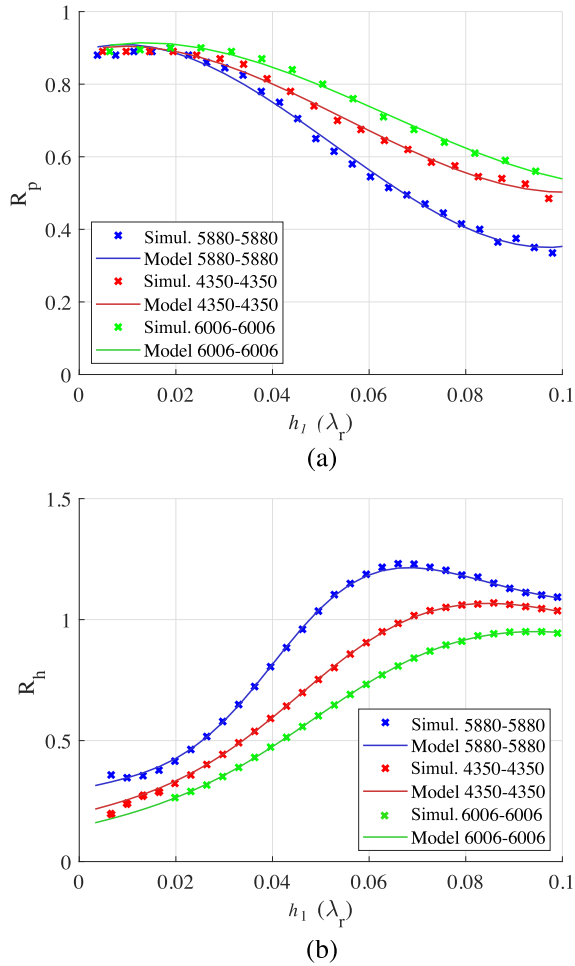
(a)



(b)

**FIGURE 2.** Comparison between the estimated and simulated values of: (a) $R_p$, and (b) $R_h$.

4350B, and 158 mils in Rogers 6006$^{\text{TM}}$ all at 3 GHz). In all the cases, it has been verified that $W_f < W_p$ and $W_f < 0.25\lambda_r$ when simulating the antenna geometry at *S*-band (2-4 GHz).

From the above equations and Fig. 2(a), it is found that the length of the feeding transmission line is more than half of the antenna length, and it tends to reduce as thicker are the substrates. It is also observed that the slope, thus $R_p$ change per $h_{1\lambda_r}$ length unit, is decreased as the permittivity is increased. In order to eventually work in a dual port with differential feeding, $R_p$ should be less than 0.5, that can happen at thicker substrates as lower permittivities have the feed substrate.

### 2) TOTAL SUBSTRATE THICKNESS
The total thickness $h_T = h_1 + h_2$ of the antenna in its optimum configuration can be calculated as:

$$h_T = h_1\left(1 + \frac{h_2}{h_1}\right) = h_1(1 + R_h) \qquad (8)$$

where the ratio $R_h$, which quantifies the relationship between the patch substrate thickness ($h_2$) and the feed substrate thickness ($h_1$) for maximizing bandwidth, can be modeled through the equations bellow. Fig. 2(b) provides an illustration of

these equations.

$$R_h = y_1 + y_2 \tanh\left(y_3(h_{1_{\lambda_r}} - y_4)\right) + y_5 \cos\left(y_6\, h_{1_{\lambda_r}}\right) \quad (9)$$

where $y_1$, $y_2$, $y_3$, $y_4$, $y_5$ and $y_6$ can be obtained using:

$$y_1 = 1.379e^{-0.7\varepsilon_r} + 0.3682 \qquad (10)$$

$$y_2 = 0.5182e^{-0.4078\varepsilon_r} + 0.6912 \qquad (11)$$

$$y_3 = 128e^{-0.925\varepsilon_r} + 25.4 \qquad (12)$$

$$y_4 = -0.0446e^{-0.6077\varepsilon_r} + 0.05295 \qquad (13)$$

$$y_5 = 0.2694e^{-0.15\varepsilon_r} + 0.2903 \qquad (14)$$

$$y_6 = 96.43e^{-0.9577\varepsilon_r} + 16.98 \qquad (15)$$

Regarding the variations of this ratio over different relative permittivities, it is noticed that the majority of cases get the best coupling as $R_h < 1$, thus $h_2 < h_1$. Notice that the actual $h_2$ used in a design may be more or less than $h_1$, $R_h$, but the coupling would be reduced, affecting mainly the bandwidth. Besides, this ratio can get a maximum value, and this peak is inversely dependent on the permittivity, but once again, these cases where $h_2 > h_1$ are only possible if $\varepsilon_r < 5.38$, according to the presented equations. It is important also to observe that it can get a value equal to one (thus, $h_2 = h_1$) as lower permittivities have both layers, which may be helpful in fabrication and logistics. As it is observed so far, this work contributes with the completion of the design of a PC-MSPA through the closed forms of the patch substrate thickness and the feeding structure dimensions.

### 3) PATCH DIMENSIONS
The square patch can be initially designed from the rectangular patch dimensions ($L_{po}, W_{po}$) as a start point. These initial dimensions can be obtained from [5] considering the total thickness $h_T$ from Eq. 8, and then, the patch dimensions can be squared by making $W_p = L_p = W_{po}$.

### B. CLOSE FORM FOR THE PC-MSPA BANDWIDTH
The impedance bandwidth is normally defined as the range of frequencies $f_l$ (lower freq.), $f_u$ (upper freq.) over which the return loss is acceptable (typically more than 10 dB ($|S_{11}| < -10$ dB)). However, the percentage (fractional) bandwidth is determined by the ratio between the impedance bandwidth and the central frequency $f_c$. Then, the percentage bandwidth is defined as:

$$\%BW = 100\frac{f_u - f_l}{f_c} = 200\frac{f_u - f_l}{f_u + f_l} \qquad (16)$$

It can be estimated from the substrates thicknesses and relative permittivities, considering that the patch and the transmission line feed are set to match the designed frequency ($L_0 = R_p L_p$, $f_c \approx f_\circ$). Then, the percentage bandwidth of the PC-MSPA with linear polarization can be predicted to be:

$$\%BW = A_{BW}\sqrt{1 - \frac{Y_8^2}{K_8^2}} \pm \Delta\%BW \qquad (17)$$

Considering that the design assumes feed substrate with thickness $h_1$ and patch substrate with thickness $h_{2_d}$, where
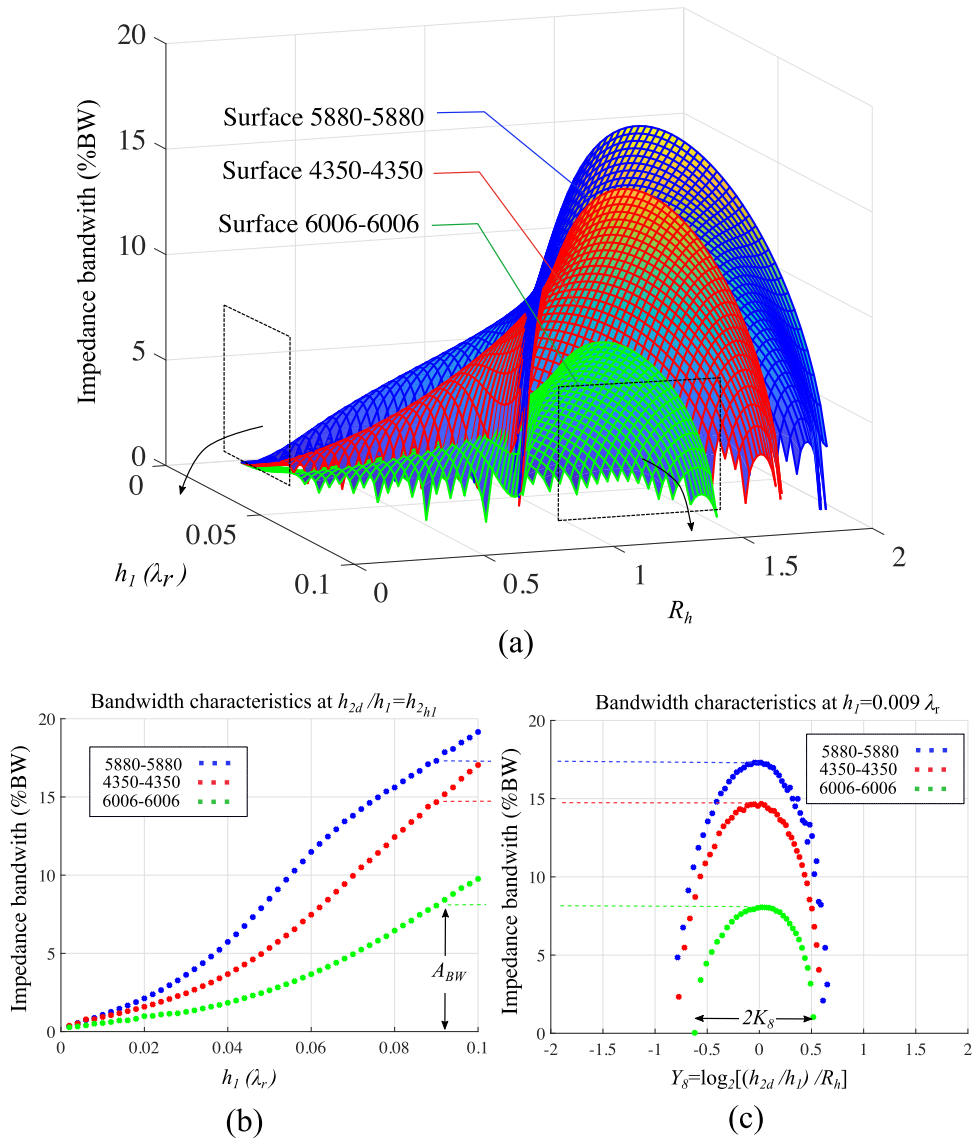
**FIGURE 3.** Bandwidth model and its side view projections, from where the terms $A_{BW}$, $Y_8$ and $K_8$ are illustrated.

$h_{2_d}/h_1$ can be different from $R_h$ of Eq. (9), and assuming equal permittivities ($\varepsilon_1 = \varepsilon_2 = \varepsilon_r$). Then, each term of Eq. (17) is expressed as:

$$A_{BW} = a_1 \left[ h_{1_{\lambda_r}}^2 - \frac{1}{2} \left( 1 + \tanh \frac{h_{1_{\lambda_r}} - a_2}{10^{-3}} \right) (h_{1_{\lambda_r}} - a_2)^2 \right] \quad (18)$$

where $a_1$, $a_2$, $K_8$ and $K_a$ can be obtained using:

$$a_1 = 98840 e^{-2.145\sqrt{\varepsilon_r}} + 533.6 \quad (19)$$

$$a_2 = -0.3252 e^{-0.8037\sqrt{\varepsilon_r}} + 0.1231 \quad (20)$$

$$K_8 = \log_2 K_{BW} = \log_2 \left[ \frac{K_a}{R_h} + \sqrt{4 + \left( \frac{K_a}{R_h} \right)^2} \right] - 1 \quad (21)$$

$$K_a = k_1 + k_2 \tanh(k_3(h_{1_{\lambda_r}} - k_4)) + k_5 \cos(k_6 h_{1_{\lambda_r}}) \quad (22)$$

where $k_1$, $k_2$, $k_3$, $k_4$, $k_5$, $k_6$, and $Y_8$ can be obtained using:

$$k_1 = 0.7682 e^{-0.3526\varepsilon_r} + 0.4086 \quad (23)$$

$$k_2 = 2.299 e^{-0.5975\varepsilon_r} + 0.2538 \quad (24)$$

$$k_3 = 80.32 e^{-1.028\varepsilon_r} + 42.36 \quad (25)$$

$$k_4 = -0.06715 e^{-0.771\varepsilon_r} + 0.04963 \quad (26)$$

$$k_5 = 1.271 e^{-0.5736\varepsilon_r} + 0.07257 \quad (27)$$

$$k_6 = 311.6 e^{-1.406\varepsilon_r} + 18.96 \quad (28)$$

$$Y_8 = \log_2 \left( \frac{h_{2_d}/h_1}{R_h} \right) \quad (29)$$

The equations expressed above for estimating the percentage bandwidth of the PC-MSPA can be summarized in three components: bandwidth amplitude $A_{BW}$, substrate allowable range $K_8$, and normalized substrate thickness ratio $Y_8$. The graphical representation of these equations are illustrated in Fig. 3. Also, there is a term of error $\Delta\%BW$, which is analyzed with more detail in Section V.

As a consequence, the formula of the bandwidth of Eq. (17) could be modeled as family of semi-elliptical curves, where
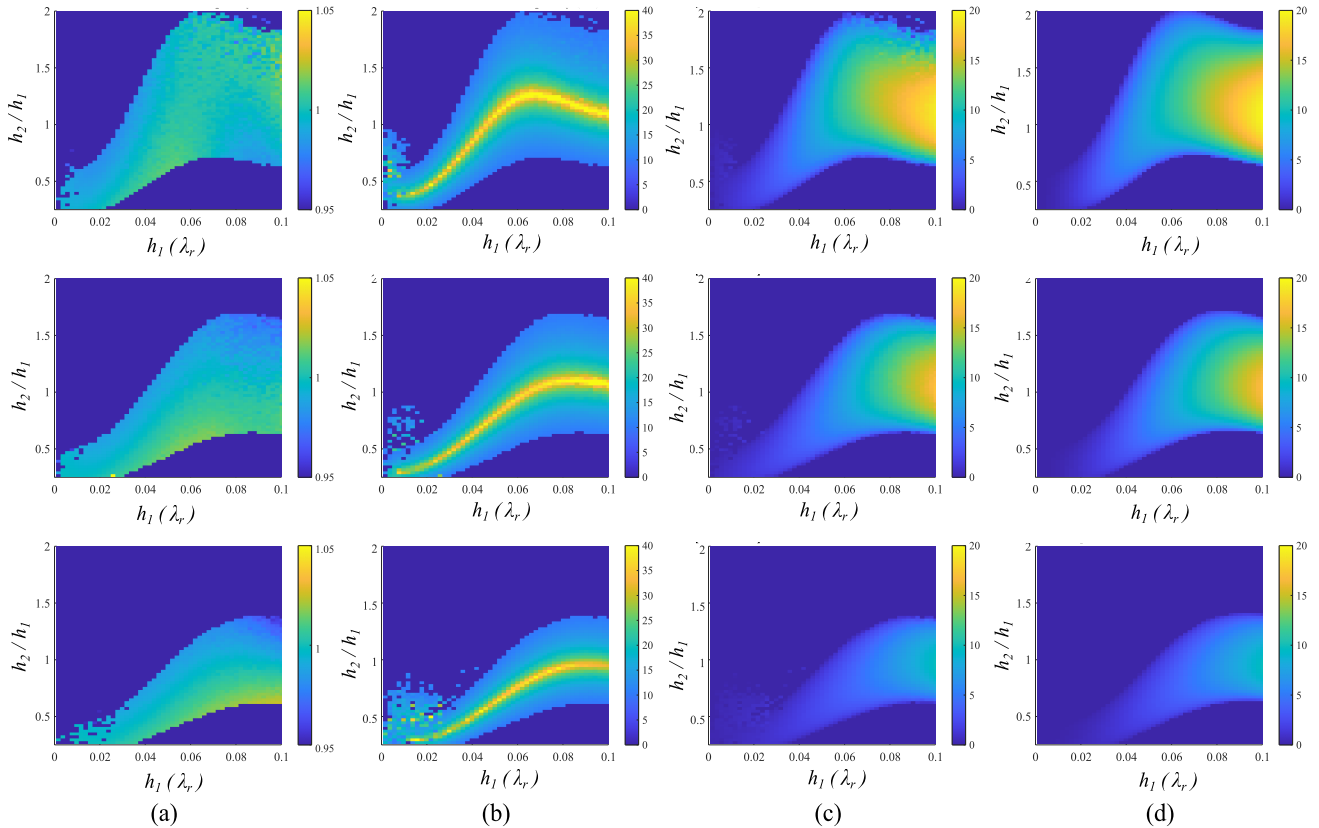
**FIGURE 4.** Antenna response for the PC-MSPA with different materials: Rogers[TM] 5880 Duroid (top row), Rogers[TM] 4350B (middle row) and Rogers[TM] 6006 (bottom row). All the variations are simulated at 3 GHz in $\lambda_o/2$ unit cell ($L_g$ = 5 cm). (a) Normalized central frequency, (b) Return loss at the central frequency ($f_c$), (c) Simulated percentage bandwidth, and (d) Modeled percentage bandwidth.

the families are conformed by $h_{1_{\lambda_r}}$ variations and each semi-ellipse has a height $A_{BW}$, a width 2 $K_8$, and they are centered in $Y_8$.

Further than the mathematical representation, the equations may be physically interpreted as the permittivities and substrate thickness change. As the permittivity increases, the bandwidth tends to reduce, and it is observed in the $A_{BW}$ term, which also has a quadratic-linear growth as the feeding substrate becomes thicker. Meanwhile, $K_8$ which mathematically is interpreted as a shape parameter represents the range of substrate thicknesses ratio where a bandwidth can exist. Lastly, but not less important, $Y_8$ represent the deviation of substrate ratio from $R_h$. Therefore, if an antenna with certain feeding substrate thickness $h_1$ has patch substrate thickness $h_{2_d} = h_1 R_h$, then it would have the maximum bandwidth, as $Y_8 = 0$. Notice that $K_8$ and $Y_8$ are in logarithmic space (octaves) and not in arithmetic progression.

## IV. IMPLEMENTATION, MEASURED RESULTS AND VALIDATION

Full wave simulations of the antenna of Fig. 1 were performed at $f_o$ = 3 GHz, considering three different materials and changing $h_1$ from 0.002 $\lambda_r$ to $0.1\lambda_r$, $h_2$ from $0.275h_1$ to $2h_1$. The transmission line length was calculated according to Eq. 2, where $R_p$ was obtained and calculated in Eq. 3.

The results are shown in Fig. 4, as follows: the first column describes the normalized central frequency ($f_c/f_o$) that in the best case should be 1; the second column shows the return loss at the simulated value of $f_c = (f_u + f_l)/2$ where $[f_l; f_u]$ is the interval where $|S_{11}| < -10$ dB; and then the third and fourth columns display the simulated and modeled percentage bandwidth of Eq. (16) and Eq. (17), respectively. For the three different materials, the model results of the percentage bandwidth in Fig. 4(d) are in good agreement with the corresponding simulated ones shown in Fig. 4(c).

On the other hand, four antenna configurations have been fabricated and measured, using two different materials and different design frequencies in the S, C and X bands. These cases have been labeled as 'Case 1', 'Case 2', 'Case 3' and 'Case 4', which specifications are listed in Table 1, noticing that $R_h = 1$ in all the cases. The simulated and measured reflection coefficients in (dB) of these antennas are shown in Fig. 5. The antenna in Case 1 and Case 4 has a ground plane size of $\lambda_o/2 \times \lambda_o/2$ where $\lambda_o$ is the free space wavelength of the design frequency. However, it is important to mention that the ground plane in the antennas of Case 2 and Case 4 has been extended to 5 cm ($\lambda_o/2$ at 3 GHz), in order to facilitate the connections for measurements. From Fig. 5, it is clear that the measured results mostly agree and validate the results produced via simulations for all cases. A small discrepancy
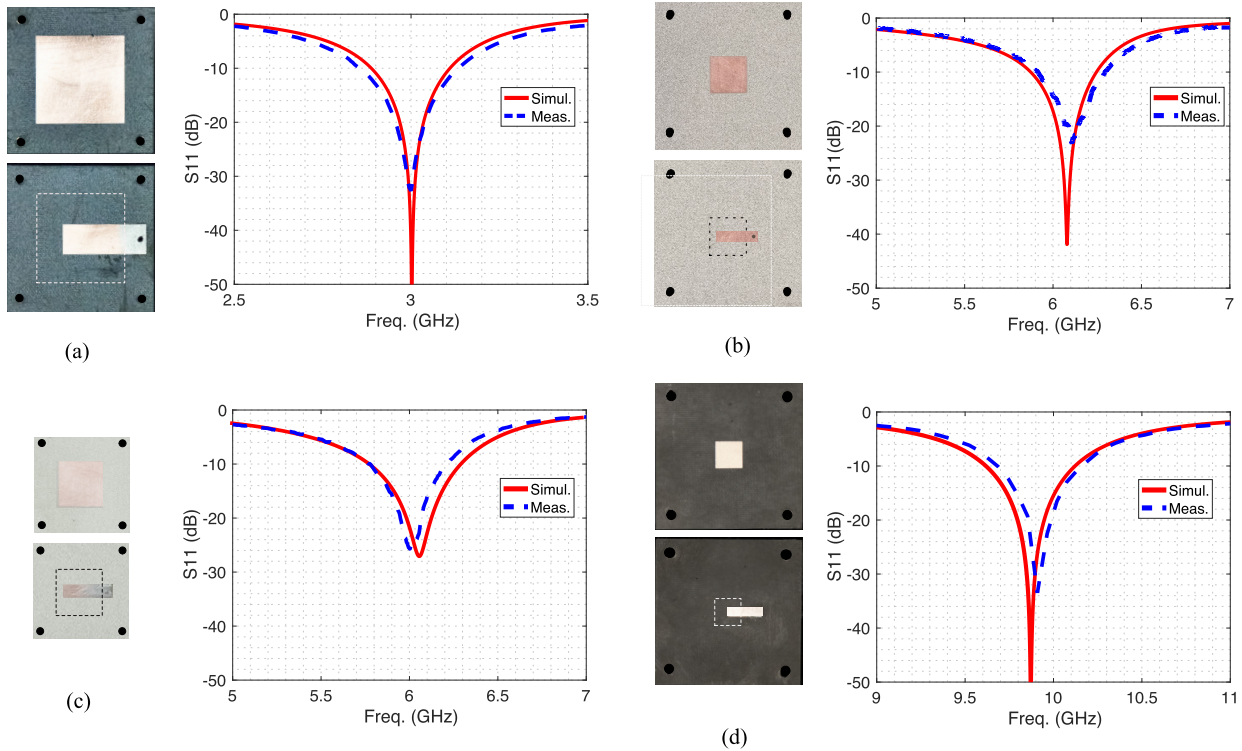
**FIGURE 5.** Measured and simulated $S11(dB)$ over frequency for: (a) Case 1: S-band PC-MSPA, (b) Case 2: C-band PC-MSPA, (c) Case 3: C-band PC-MSPA, and (d) Case 4: X-band PC-MSPA.

**TABLE 1.** Fabricated antennas' specifications.

| Parameters | Units | Case 1 | Case 2 | Case 3 | Case 4 |
|---|---|---|---|---|---|
| $f_o$ | GHz | 3 | 6 | 6 | 10 |
| $\varepsilon_1, \varepsilon_2$ | - | 2.20 | 3.48 | 3.48 | 2.20 |
| $h_1, h_2$ | mm | 3.175 | 1.524 | 1.524 | 0.790 |
| $L_p, W_p$ | mm | 29.40 | 11.82 | 11.80 | 9.070 |
| $L_g, W_g$ | mm | 50.00 | 50.00 | 2.000 | 50.00 |
| $R_p$ | - | 0.686 | 0.687 | 0.721 | 0.760 |
| $L_f$ | mm | 27.87 | 13.27 | 12.68 | 11.50 |
| $W_f$ | mm | 10.00 | 3.350 | 3.350 | 2.420 |
| $L_s$ | mm | 1.800 | 1.500 | 1.500 | 1.500 |
| $L_o$ | mm | 20.56 | 7.680 | 7.100 | 4.530 |

**TABLE 2.** Errors between the proposed model and both simulation and measurement.

| Case | $f_c$ | $\%(\Delta f_c)/f_c$ | | $\Delta\%BW$ | |
|---|---|---|---|---|---|
| | | Measured | Simulated | Measured | Simulated |
| Case 1 | 3 GHz | 0.17 | 0.04 | 1.41 | 0.18 |
| Case 2 | 6 GHz | 1.91 | 0.99 | 0.80 | 0.98 |
| Case 3 | 6 GHz | 0.09 | 0.76 | 0.15 | 1.46 |
| Case 4 | 10 GHz | 1.00 | 1.30 | 0.65 | 0.39 |

between the simulated and measured results may be caused by the error of the fabrication and assembling of the antenna.

Furthermore, an analysis of model errors is presented through the plots in Fig. 6. The plot in Fig. 6(a) shows the percentage RMSE error of the central frequency in the simulation results with respect to the intended central frequency, which is expressed as $\Delta f_c/f_c$. Meanwhile, Fig. 6(b) shows the bandwidth error term in Eq. (17), which is calculated as $\Delta\%BW = |\%BW_{modeled} - \%BW_{simulated}|$ from Fig. 4.

## V. ERROR ANALYSIS

Table 2 quantifies the errors between simulated, measured with calculated results using the proposed method described in Section III. For all cases this error analysis was performed using the central frequency ($f_c$) and frequency band ($BW$) for each prototype.

The central frequency in all simulated cases are around the design operation frequency, having an root mean square error (RMSE) less than 5% (1.34% in Rogers 5880, 1.45% in Rogers 4350, and 2.76% in Rogers 6006), as noticed in the color space in the first column of Fig. 4. This high agreement is due to the accurate design from Eq. (2). However, in the same figure, it is seen that for very thin antennas ($h_1 < 0.03\lambda_r$, $h_{2d}/h_1 < 0.75$), the normalized central frequency $f_c/f_o$ is less than 0.95 (dark blue colored in the first column that are not in the other columns), reflecting also in the higher RMSE as shown in Fig. 6(a). These fluctuations are primarily due to the numerical simulation errors for very thin substrates. On the other hand, as the feed thickness $h_1$ increases ($h_1 > 0.03\lambda_r$), the percentage RMSE go down to less than 5%. Meanwhile, according to Table 2, the measured central frequency in the four cases also have a very good agreement, having slightly more errors in Case 2 and Case 4, due to fabrication imperfections.

The maximum return loss, and maximum predicted bandwidth, are obtained when the parameter $Y_8 = 0$ in Eq. (17),

**TABLE 3.** A comparison between the proposed model for PC-MSPA bandwidth and available models for MSPA bandwidth ($h_1 = h_2$, $L_p = W_p$).

| Parameters | Reference (HFSS) | Bandwidth (Error) | Theoretical Bandwidth Estimation | | | |
|---|---|---|---|---|---|---|
| | | | **Proposed Model** | Previous Work | | |
| | | | | Ref. [24] | Ref. [25] | Ref. [26] |
| $f_o$=3 GHz, $\varepsilon_r$=2.20 $h_1$=125 mils, $W_p$=29.40 mm | 7.430 | %BW | **7.610** | 6.433 | 7.706 | 9.600 |
| | | ($\Delta_{BW}$) | **(0.180)** | (0.997) | (0.276) | (2.170) |
| $f_o$=10 GHz, $\varepsilon_r$=6.15 $h_1$=50 mils, $W_p$=4.85 mm | 10.28 | %BW | **10.37** | 4.323 | 6.145 | 12.80 |
| | | ($\Delta_{BW}$) | **(0.090)** | (5.959) | (4.317) | (2.518) |
| $f_o$=10 GHz, $\varepsilon_r$=3.48 $h_1$=60 mils, $W_p$=6.28 mm | 16.38 | %BW | **16.32** | 7.963 | 10.89 | 15.36 |
| | | ($\Delta_{BW}$) | **(0.060)** | (8.417) | (5.487) | (1.020) |
| $f_o$=6 GHz , $\varepsilon_r$=2.20 $h_1$=125 mils, $W_p$=12.19 mm | 17.79 | %BW | **18.17** | 13.64 | 18.84 | 19.20 |
| | | ($\Delta_{BW}$) | **(0.385)** | (4.149) | (1.052) | (1.415) |

which means $h_{2_d} = h_1 R_h$. This has been verified through the comparison between the simulations of Fig. 4(b) and the frequency responses of Fig. 5. Considering Case 1 and Case 3, which do not have a ground plane extension, the values of $|Y_8|$ are 0 and 0.17, meaning that the return loss would be stronger in Case 1 than in Case 3. This behavior is clearly observed in the simulation and experiment as shown in Fig. 5(a) and Fig. 5(c).

Regarding the antenna bandwidth, the RMSE of the term %$\Delta BW$ is less than 2, as observed in Fig. 6(b), showing high accuracy of the model in comparison with the simulation. These errors remain the same over $h_{1_{\lambda_r}}$, but they represent a bigger relative error when $h_{1_{\lambda_r}}$ is small, i.e. less than $0.03\lambda_r$, being observed, e.g in the dusty area in the bottom-left image corners in the Fig. 4(b), where the predicted bandwidth is zero. Due to numerical fluctuations in the simulations, the term $\Delta\%BW$ may be higher at $Y_8 \approx K_8$, where the expected percentage bandwidth goes to zero. In addition, from the experimental results, it is observed in Table 2 that the bandwidth has an error term up to 1.46%. Overall, the expression of the bandwidth can get a good estimation of the bandwidth, but it should be considered only as a reference value, as it may differ from measured values due to fabrication errors and limitations, as well as numerical errors especially in very thin antennas.

Those results mean that the proposed model of $R_p$ allows to have a PC-MSPA with an stabilized central frequency and around the design frequency of the antenna. The maximum return loss and bandwidth results show that the model and prediction have good agreement with results, but the model errors may increase as more modifications the antenna has, and as $h_{2_d}/h_1$ is far away from the $R_h$, affecting the maximum return loss and bandwidth as well. In that sense, in order to increase the bandwidth, it is observed that feed substrates with higher thickness would allow to reach this purpose, as long as the patch substrate has the appropriate dimension related to $R_h$ in order to maximize coupling.

In addition, the proposed model is compared with other models available in literature [24]–[26]. The calculated percentage bandwidths for electrically thin and thick PC-MSPA



(a)



(b)
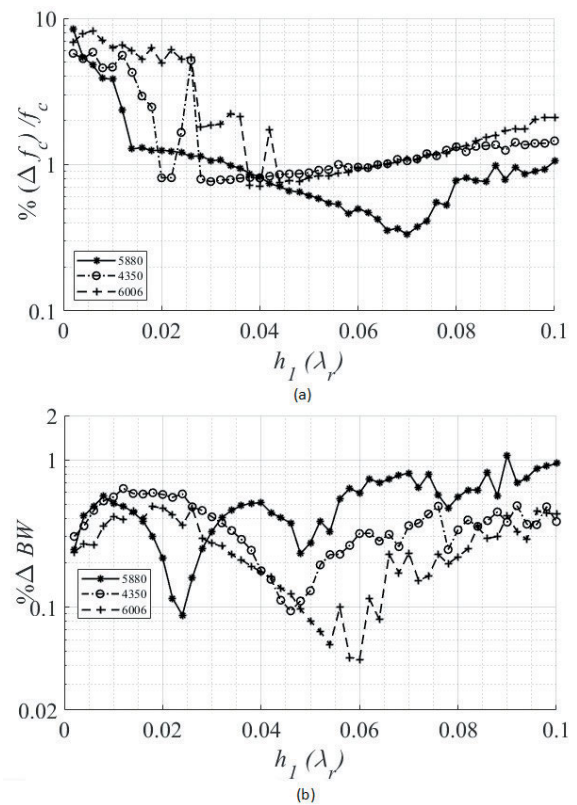
**FIGURE 6.** RMSE model errors over $h1_{\lambda_r}$: (a) Central frequency fluctuations, (b) Percentage bandwidth term %$\Delta BW$.

antennas with different physical dimensions and substrates are compared with those from HFSS simulations and other models. Four cases of study are used and listed in Table 3, considering the simulated value of the PC-MSPA bandwidth as a reference. It is seen from Table 3 that when the substrate electrically thickness like Case 2 and Case 3, the error between the simulated and predicated bandwidth is less than 0.1% using the new model. However, as expected other models have higher errors; in some of them, the error is about 10%. For electrically thin substrates, Case 1 and Case 4, the new model generally has better performance even though other models have comparable results.

## VI. CONCLUSION

This paper has provided a new set of equations to compute the bandwidth of a proximity-coupled square microstrip patch antenna (PC-MSPA). The proposed model is used for two layers (thin or thick) PC-MSPA. A extensive mathematical analysis of this antenna has been undertaken at several levels of design complexity to evaluate the robustness of proposed expressions. Generic expressions used to calculate impedance bandwidth of edge and probe-fed microstrip patch antennas has been discussed and compared with proposed model. Although those expressions can be used for PC-MSPA, those does not provide accurate estimation of bandwidth of a PC-MSPA. Four PC-MSPA antennas were designed, fabricated with different materials, thickness, bandwidth requirements and frequency bands. In all cases, simulated and measured results agree very well with results obtained from proposed analytical model. Errors between the proposed analytical model and both simulation and measurement are less than 3.1%. The proposed models are mostly valid for permittivities between 2.2 and 6.15, and with feed substrate thickness less than $0.1\lambda_r$.

## ACKNOWLEDGMENT

## REFERENCES

[1] A. G. Deschamps, "Microstrip microwave antennas," in *Proc. 3rd USAF Symp. Antennas*, 1953.

[2] H. Gutton and G. Baissinot, "Flat aerial for ultra high frequencies," French Patent 703 113, 1955.

[3] R. Munson, "Conformal microstrip antennas and microstrip phased arrays," *IEEE Trans. Antennas Propag.*, vol. AP-22, no. 1, pp. 74–78, Jan. 1974.

[4] J. W. Howell, "Microstrip antennas," *IEEE Trans. Antennas Propag.*, vol. AP-23, no. 1, pp. 90–93, Jan. 1975.

[5] C. A. Balanis, *Antenna Theory: Analysis and Design*. Hoboken, NJ, USA: Wiley, 2015.

[6] K. F. Lee, *Microstrip Patch Antennas*. London, U.K.: Imperial College Press, 2011.

[7] P. Bhartia, I. Bahl, R. Garg, and A. Ittipiboon, *Microstrip Antenna Design Handbook*. London, U.K.: Artech House, 2001.

[8] D. Pozar and D. Schaubert, *Microstrip Antennas: The Analysis and Design of Microstrip Antennas and Arrays*. New York, NY, USA: IEEE Press, 1995.

[9] K. R. Carver and J. W. Mink, "Microstrip antenna technology," *IEEE Trans. Antennas Propag.*, vol. AP-29, no. 1, pp. 2–24, Jan. 1981.

[10] E. Van Lil and A. Van De Capelle, "Transmission line model for mutual coupling between microstrip antennas," *IEEE Trans. Antennas Propag.*, vol. AP-32, no. 8, pp. 816–821, Aug. 1984.

[11] Y. T. Lo, D. Solomon, and W. F. Richards, "Microstrip microwave antennas," *IEEE Trans. Antennas Propag.*, vol. AP-27, pp. 137–145, 1979.

[12] W. F. Richards, Y. T. Lo, and D. D. Harrison, "An improved theory for microstrip antennas and applications," *IEEE Trans. Antennas Propag.*, vol. AP-29, no. 1, pp. 25–27, Jan. 1981.

[13] V. Palanisamy and R. Garg, "Analysis of arbitrarily shaped microstrip patch antennas using segmentation technique and cavity model," *IEEE Trans. Antennas Propag.*, vol. AP-34, no. 10, pp. 1208–1213, Oct. 1986.

[14] M. Davidovitz and Y. T. Lo, "Rigorous analysis of a circular patch antenna excited by a microstrip transmission line," *IEEE Trans. Antennas Propag.*, vol. 37, no. 8, pp. 949–958, 1989.

[15] M.-J. Tsai, F. De Flaviis, O. Fordham, and N. G. Alexopoulos, "Modeling planar arbitrarily shaped microstrip elements in multilayered media," *IEEE Trans. Microw. Theory Techn.*, vol. 45, no. 3, pp. 330–337, Mar. 1997.

[16] F. Alonso-Monferrer, A. kishk, and A. Glisson, "Green's functions analysis of planar circuits in a two-layer grounded medium," *IEEE Trans. Antennas Propag.*, vol. 40, no. 6, pp. 690–696, Jun. 1992.

[17] D. Pozar and S. Voda, "A rigorous analysis of a microstripline fed patch antenna," *IEEE Trans. Antennas Propag.*, vol. AP-35, no. 12, pp. 1343–1350, Dec. 1987.

[18] G. Splitt and M. Davidovitz, "Guidelines for design of electromagnetically coupled microstrip patch antennas on two-layer substrates," *IEEE Trans. Antennas Propag.*, vol. 38, no. 7, pp. 1136–1140, Jul. 1990.

[19] D. M. Pozar and B. Kaufman, "Increasing the bandwidth of a microstrip antenna by proximity coupling," *Electron. Lett.*, vol. 23, no. 8, pp. 368–369, 1987.

[20] K. Lee, Fong, and K.-F. Tong, *Microstrip Patch Antennas*. Singapore: Springer, 2016, pp. 787–852.

[21] R. P. Parrikar and K. C. Gupta, "Multiport network model for CAD of electromagnetically coupled microstrip patch antennas," *IEEE Trans. Antennas Propag.*, vol. 46, no. 4, pp. 475–483, Apr. 1998.

[22] H. F. Pues and A. R. Van de Capelle, "An impedance-matching technique for increasing the bandwidth of microstrip antennas," *IEEE Trans. Antennas Propag.*, vol. 37, no. 11, pp. 1345–1354, Nov. 1989.

[23] M. P. David, D. Pozar, and D. Schaubert, "A review of bandwidth enhancement technique for microstrip antennas," in *Microstrip Antennas: The Analysis and Design of Microstrip Antennas and Arrays*. Piscataway, NJ, USA: IEEE Press, 1995, pp. 157–166.

[24] D. R. Jackson and N. G. Alexopoulos, "Simple approximate formulas for input resistance, bandwidth, and efficiency of a resonant rectangular patch," *IEEE Trans. Antennas Propag.*, vol. 39, no. 3, pp. 407–410, Mar. 1991.

[25] G. Kumar and I. Ray, *Broadband Microstrip Antennas*. London, U.K.: Artech House, 2003.

[26] R. C. Johnson, *Antenna Engineering Handbook*. New York, NY, USA: McGraw-Hill, 1993.

[27] N. Kumprasert, C. Namkang, and T. Tassri, "Parametric study of the rectangular microstrip antenna with an air gap," *KMUTT Res. Develop. J.*, vol. 24, no. 1, pp. 131–142, 2001.

[28] S. A. R. Parizi, "Bandwidth enhancement techniques," in *Trends in Research on Microstrip Antennas*. Rijeka, Croatia: InTech, 2017.

[29] S. M. Duffy, "An enhanced bandwidth design technique for electromagnetically coupled microstrip antennas," *IEEE Trans. Antennas Propag.*, vol. 48, no. 2, pp. 161–164, 2000.

[30] S. L. Arlinghaus, *Practical Handbook of Curve Fitting*. Boca Raton, FL, USA: CRC Press, 1994.

[31] R. Garg, I. Bahl, and M. Bozzi, *Microstrip Lines and Slotlines*. Norwood, MA, USA: Artech House, 2013.
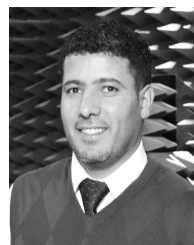
**NAFATI ABOSERWAL** (Member, IEEE) received the B.S. degree in electrical engineering from Al-Mergheb University, Alkhoms, Libya, in 2002, and the M.S. and Ph.D. degrees in electrical engineering from Arizona State University, Tempe, AZ, USA, in 2012 and 2014, respectively. In January 2015, he joined the Advanced Radar Research Center (ARRC), The University of Oklahoma (OU), Norman, and the Department of Electrical and Computer Engineering, OU, as a Postdoctoral Research Scientist. He is currently a Research Associate and a Manager of far-field, near-field and environmental anechoic chambers with the Radar Innovations Laboratory (RIL), OU. His research interests include EM theory, computational electromagnetics, antennas, and diffraction theory, edge diffraction, and discontinuities impact on the array performance. His research also focuses on active high performance phased array antennas for weather radars, higher modes and surface waves characteristics of printed antennas, and high performance dual-polarized microstrip antenna elements with low cross-polarization. He is a member of the IEEE TRANSACTIONS ON ANTENNAS AND PROPAGATION.
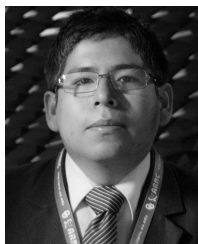
**NIM R. CCOILLO RAMOS** (Student Member, IEEE) received the B.Sc. and M.Sc. degrees in electronics engineering from the Universidad Nacional de Ingenieria (UNI), Lima, Peru, in 2016 and 2018, respectively. He is currently pursuing the Ph.D. degree in electrical and computer engineering with The University of Oklahoma (OU), USA, researching in electromagnetic antenna modeling for phased arrays in the Advanced Radar Research Center. At the end of his undergraduate studies, he joined the National Institute of Research and Training in Telecommunications (INICTEL-UNI), Lima, where he is working as an Intern in electronics engineering with focus on electromagnetics and after graduate studies, as a Research Assistant. During his graduate studies, he worked in X-and-P-band radar image processing to estimate forest changes in the Amazon, having a six month stay with the Department of Telecommunications, State University of Campinas, Brazil.

**ZEESHAN QAMAR** (Member, IEEE) received the B.Sc. and M.Sc. degrees in electrical engineering from COMSATS University, Islamabad, Pakistan, in 2010 and 2013, respectively, and the Ph.D. degree in electronic engineering from the City University of Hong Kong, Hong Kong, in 2017. From July 2010 to August 2013, he was a Research Associate with the Department of Electrical and Computer Engineering, COMSATS University. From November 2017 to April 2018, he was a Postdoctoral Research Associate with the Department of Materials Science and Engineering, City University of Hong Kong. He is currently a Postdoctoral Research Fellow with the Phased Array Antenna Research and Development group (PAARD), The University of Oklahoma, Norman, OK, USA, and the Advanced Radar Research Center (ARRC), The University of Oklahoma. His current research interests include microwave/millimeter-wave circuits, material characterization, meta-materials, artificial dielectric layer, antennas and phased arrays, and phased array antennas. He is a member of the IEEE Antennas and Propagation Society (AP-S), and a Reviewer of various IEEE and IET conferences and journals.

**JORGE L. SALAZAR-CERRENO** (Senior Member, IEEE) received the B.S. degree in ECE from University Antenor Orrego, Trujillo, Peru, the M.S. degree in ECE from the University of Puerto Rico, Mayagüez (UPRM), and the Ph.D. degree in ECE from the University of Massachusetts Amherst, Amherst, in 2011. His Ph.D. research focused on development of low-cost dual-polarized active phased array antennas (APAA). After graduation, he received the prestigious National Center for Atmospheric Research (NCAR) Advanced Study Program (ASP) Postdoctoral Fellowship. At NCAR, he worked at the Earth Observing Laboratory (EOL) Division, where he is developing airborne technology for two-dimensional, electronically scanned, and dual-pol phased array radars for atmospheric research. In July 2014, he joined the Advanced Radar Research Center (ARRC), The University of Oklahoma, as a Research Scientist, and became an Assistant Professor with the School of Electrical and Computer Engineering in August 2015. His research interests include high-performance, broadband antennas for dual-polarized phased array radar applications, array antenna architecture for reconfigurable radar systems, APAA, Tx/Rx modules, radome EM modeling, and millimeter-wave antennas. He is a Senior Member of the IEEE Antennas and Propagation Society (AP-S). In 2019, he received the prestigious William H. Barkow Presidential Professorship from The University of Oklahoma for meeting the highest standards of excellence in scholarship and teaching. He is a Reviewer of various IEEE and AMS conferences and journals.

● ● ●